Accepted Manuscript

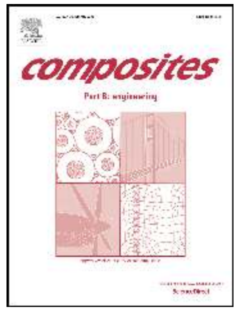

Experimental study of flexural behaviour of RC beams strengthened by longitudinal and U-shaped basalt FRP sheet

Wensu Chen, Thong M. Pham, Henry Sichembe, Li Chen, Hong Hao

PII: S1359-8368(17)30651-0

DOI: 10.1016/j.compositesb.2017.09.053

Reference: JCOMB 5300

To appear in: *Composites Part B*

Received Date: 22 February 2017

Revised Date: 25 September 2017

Accepted Date: 25 September 2017

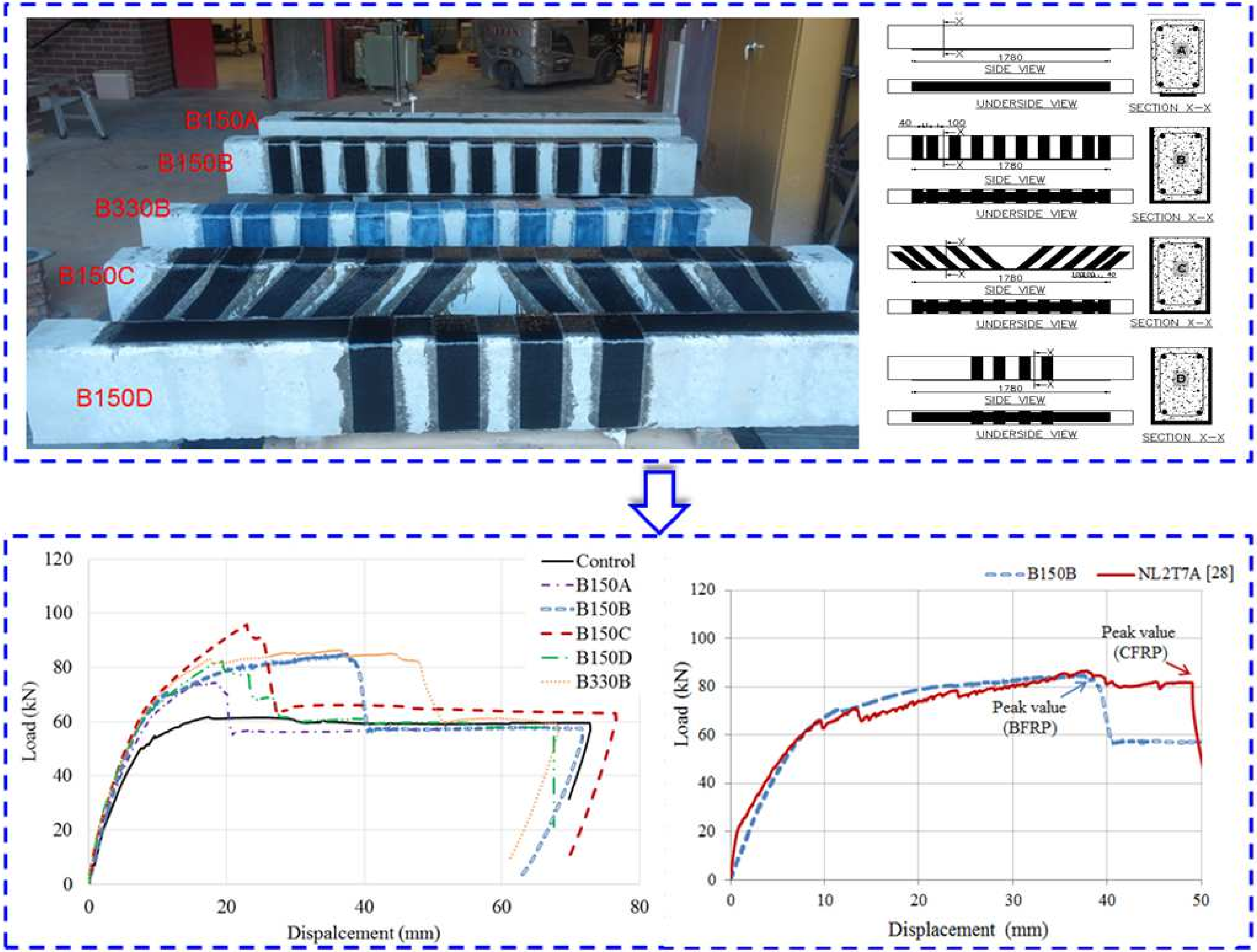
B150A
B150B
B330B
B150C
B150D
1780
SIDE VIEW
UNDERSIDE VIEW
SECTION X–X
Control
B150A
B150B
B150C
B150D
B330B
Load (kN)
Dispalcement (mm)
B150B
NL2T7A [28]
Peak value (CFRP)
Peak value (BFRP)
Load (kN)
Displacement (mm)

Experimental Study of Flexural Behaviour of RC Beams Strengthened by Longitudinal and U-shaped Basalt FRP Sheet

Wensu Chen[1], Thong M. Pham[1], Henry Sichembe[1], Li Chen[2] and Hong Hao[1]*

[1]*Centre for Infrastructural Monitoring and Protection,*

School of Civil and Mechanical Engineering, Curtin University, Australia

[2]*PLA University of Science and Technology, Nanjing, 210007, China*

[*] Corresponding author's email: hong.hao@curtin.edu.au

Abstract

Fiber Reinforced Polymer (FRP) composite products such as Carbon FRP (CFRP) or Glass FRP (GFRP) have been intensively studied for strengthening reinforced concrete (RC) and masonry structures. It has been reported that FRP strengthening is effective to enhance the structural load-carrying capacity. Basalt FRP (BFRP) is a promising material for the application to structure strengthening with its advantages of low cost, corrosion resistant and sound mechanical property, but only limited studies of using Basalt FRP to externally strengthen RC beam are available in the literature. This study is to experimentally explore the effectiveness of application of Basalt FRP to strengthen RC beam under three-point bending test. The damage modes and

structural response of unstrengthened and BFRP strengthened RC beams were recorded and identified. The effects of various BFRP wrapping schemes, U-jacket anchorage and epoxy adhesives on the flexural capacity of RC beams were analysed and discussed. In addition, the formulae used to predict the flexural behaviour of RC beam strengthened by other FRP composites (e.g. CFRP/GFRP) were evaluated for their applicability to Basalt FRP strengthening.

Keywords: Basalt FRP (BFRP), U-jacket, flexural, strengthening

1 Introduction

The use of FRP composites for structural strengthening was initiated in the late 1980s. FRP has some advantages over traditional steel plates, such as high strength to weight ratio, resistance to corrosion, flexibility and overall versatility [1]. The most commonly used FRP in the industry is made of mainly carbon fibre (CFRP), glass fibre (GFRP), aramid fibre (AFRP) and basalt fibre (BFRP). Various fibre composites have been used to repair or strengthen structural components. Huang, et al. [2] investigated the flexural behaviour of RC beams externally strengthened by natural flax FRP composite. Dong, et al. [3] studied the flexural and flexural-shear strengthening capacities of RC beams externally strengthened with FRP sheets. It was found that flexural-shear strengthening scheme was more effective than the flexural one in improving the stiffness and ultimate strength of RC beam. Choi, et al. [4] reported debonding behaviour and structural performance of RC beams strengthened by hybrid FRP composites. Skuturna and Valivonis [5] investigated the FRP strengthening effect and failure modes of RC beams using various anchorage systems. Yu and Wu [6] reported the performance of cracked steel beams reinforced by normal modulus CFRP with different patch systems. Nguyen, et al. [7] used textile-reinforced concrete to strengthen structural components of existing structures. Basalt fibre is an environmentally friendly material which is made from melted basalt rock under high temperature of 1400 °C and the molten rock is then extruded through small nozzles to produce the fine fibre [8]. Basalt fibre is usually manufactured in a single process known as continuous spinning, which allows for the production of short fibres and continuous fibres [8]. The fibres can be made in the forms of chopped fibres, rebars and continuous fibre sheets etc. Basalt FRP (BFRP) is a relative newcomer to FRP composites, as compared with carbon FRP (CFRP) and glass FRP (GFRP). Although it has superior characteristics such as high strength to weight ratio, sound ductility and durability, high thermal resistance, and good corrosion resistance, and is cost effective [9], its performance in structural strengthening has been less studied.

Externally bonded FRP has been intensively used in the flexural strengthening of RC beams [10-16]. The strengthening of RC structural components by using FRP laminates on the tension side has exhibited substantial enhancement to confinement, stiffness and overall load carrying capacity [17]. Attari, et al. [18] reported that the use of twin-layer GFRP sheets was effective in beam strengthening, exhibiting flexural capacity gains as high as 114%. Sen and Reddy [19] used natural jute fibre textile reinforced (JFRP) composite system to strengthen RC beams in flexure and compared the effectiveness with using CFRP and GFRP strengthening systems. It was reported that the ultimate flexural strength of the RC beams reinforced by JFRP, CFRP and GFRP could be improved by 62.5%, 150% and 125%, respectively, with full wrapping technique and by 25%, 50% and 37.5%, respectively with strip wrapping scheme. However, only limited study of using Basalt FRP as an alternative material to strengthen beam is available in literature. Sim, et al. [9] externally bonded BFRP strips to the tension side of RC beams to increase the flexural load carrying capacity. Both yielding and ultimate strength of the beam specimen increased up to 27%, depending on the number of layers applied. Şerbescu, et al. [20] investigated the use of BFRP U-jacket strips as external shear reinforcement for RC beams, showing efficiently delaying debonding failure at the plate end and reducing the brittleness of failure.

FRP debonding (i.e. detachment of FRP from the concrete substrate) at the end or intermediate crack (IC) debonding was identified as the frequently observed failure mode [21-23]. Different anchorage measures have been used to suppress various debonding failure to enhance the utilization efficiency of FRP material. Chahrour and Soudki [24] studied the flexural behavior of RC beams strengthened by CFRP with end anchorages to prevent peeling. Fu, et al. [25] externally bonded vertical and 45° inclined FRP U-jackets at the plate ends as anchorage solution to mitigate the concrete cover separation and intermediate crack debonding failure, which enhanced the load-carrying capacity and ductility of beam. Smith and Teng [26] reported using vertical FRP U-jacket at the end of the FRP soffit plate could lead to enhancement in the ultimate load but the enhancement is limited. Lee and Lopez [27] used vertical or inclined FRP U-jacket to enhance the strength of bonded joints with the range of 14% to 118%. Pham and Hao [28] reported that using FRP U-wraps maximize the capability of longitudinal FRP strips. Pham and Hao [29] investigated the effectiveness and behaviour of 45° inclined U-jackets to the enhanced ability to arrest flexural and shear cracks. Some design guidelines including ACI 440.2 R-08 [30] specify the installation of vertical FRP U-jackets at plate end anchorage to suppress concrete cover separation. However, a thorough comparison between the efficiency of vertical and inclined U-jackets has not been presented. In this study, the longitudinal and transverse strains of FRP U-jackets are presented and discussed.

As above-mentioned, basalt fibre is an alternative material for structural strengthening. However, the testing data of BFRP strengthened beam is limited [9, 20]. More testing data on BFRP strengthening is desired to supplement the current understandings for more reliable and convincing results. The efficacy of beam strengthening by using CFRP and BFRP has not been compared yet. The study on the effects of different wrapping schemes using U-jacket anchorages and epoxy adhesives on BFRP strengthening performance is limited. In addition, the design guidelines provided in ACI 440.2R-08 [30] are applicable for CFRP/GFRP/AFRP materials while its applicability of using BFRP to strengthen RC structure has not been verified yet. The verification of the predications on BFRP strengthening is thus desired.

In this study, the effectiveness of different FRP anchors and epoxy adhesives in strengthening RC beams in flexural was experimentally investigated. The changes of the failure modes and the enhancement of the load-carrying capacity of RC beams strengthened with BFRP were discussed. In addition, the design guideline proposed by ACI 440.2R-08 for predicting the flexural behaviour of RC beams strengthened with other FRP composites were evaluated against BFRP.

2 Testing schemes

2.1 Specimen design

In order to study the efficacy of BFRP strengthening beam under three-point bending, six beams including one reference beam and five strengthened beams (namely B150A, B150B, B150C, B150D and B330B) were prepared as detailed in Table 1. The dimensions of the beams were 150 mm in width, 250 mm in height and 2200 mm in length. All RC beams were reinforced with two deformed bars with 10-mm-diameter at the tension side and two 12-mm-diameter bars at the compression side of the beam in the longitudinal direction. All the six beams were designed to fail in flexural mode with 10-mm-diameter steel stirrups at a spacing of 115 mm throughout the beam, which indicated the shear resistance was much higher than the flexural resistance. The details of the reinforcement are shown in Figure 1. The ready-mixed concrete with the compressive strength of 40 MPa at 28 day age was used to cast the beams.

Based on the study conducted by Spadea, et al. [17], four wrapping schemes were employed as shown in Figure 2. Each wrapping scheme comprised of either BFRP soffit strips, U-jackets or a combination of them. In order to assess the significance of epoxy adhesive, two different epoxies were also adopted to compare. Each specimen was subjected to three point bending test until failure.

2.2 Material properties

The unidirectional BFRP sheet with the width of 100 mm and the density of 300 g/m^2 was selected as external reinforcement. The nominal thickness of the BFRP sheet was 0.12 mm. The BFRP sheet had a tensile strength of 2100 MPa, tensile modulus of 77.9 GPa, and 2.1% tensile elongation [31]. To examine the strengthening efficacy by using BFRP and CFRP, the experimental results from this study were compared with RC beams strengthened with CFRP, reported in the study by Pham and Hao [28]. Accordingly, four layers of longitudinal BFRP strip were applied to ensure the equal tensile force (i.e. width*thickness*tensile strength) provided by two layers of CFRP strips with nominal thickness of 0.45 mm, as given in Table 2.

Premature debonding failure was a major issue of FRP reinforced concrete. The most extensively used bonding agent for external FRP application was epoxy adhesive, which consisted of two parts known as resin and hardener. To investigate the effect of epoxy adhesives contributing to debonding of BFRP, two widely used epoxies i.e, SikaDur 330 and West System 105-206 were adopted. As given in Table 3, the elongation of the epoxy resin West System 105-206 was higher than that of SikaDur 330. Accordingly, FRP strengthened RC beams used West System 105-206 may provide a higher load-carrying capacity than that of the beams used SikaDur 330. However, it has been observed that debonding failure might initiate from the concrete cover which was observed from the specimen B150D of this study so that the adhesive does not necessarily govern the strength capacity of the beams. In addition, the difference in the tensile modulus and elongation may also affect the effectiveness of applying these adhesives. Therefore, the performance of using these adhesives was unknown and investigated in this study.

2.3 Specimen preparation

Stress concentration can cause FRP premature rupture and lead to a low efficiency of using FRP strengthening [32]. This phenomenon is highly dependent on the geometry of the beam because stresses concentrate at sharp edges but well distribute along gradual curves. Therefore, the edges of the beams were rounded at points which would be in contact with the U-jackets using an angle grinder. The radius of the rounded corners was about 25 mm. Careful surface preparation was carried out to remove weak concrete before bonding FRP to the beams. A pneumatic needle gun was used to carefully roughen the concrete surface. The accumulation of dust and weak concrete resulting from grinding and needling processes was removed using a pressurised air hose. The concrete surface was cleaned by acetone followed by applying primer to the concrete surface before bonding with FRP. The wet layup procedure was adopted for FRP bonding as shown in Figure 3. Prior to testing, all beams as shown in Figure 4 were allowed a minimum of seven days for the epoxy adhesive to cure.

3 Testing setup and instrumentation

The quasi-static testing setup included testing frame, A-frame supports, hydraulic jack, LVDT, data acquisition system and other equipment as shown in Figure 5. A three-point loading configuration using a roller and pin was used to provide simply supported boundary condition. The effective span of the beams was 1.9 m. The beams were loaded by using hydraulic jack with a loading rate at 0.6 mm/min. A number of linear variable differential transformers (LVDT) and strain gauges were attached to the beams at different locations to measure the deflection and strain values, respectively. The load-displacement curves for each LVDT and the strain-time histories for each strain gauge were recorded.

Debonding and rupture were two types of failure modes expected in these strengthened beams. If debonding occurs it indicates that the high tensile strength of FRP has been under-utilised. In order to monitor the longitudinal strains of BFRP, a number of strain gauges were attached to the strengthened beams at the marked locations i.e. the soffit of the beams (SGC “Strain Gauge Centre”; SGE1 “Strain

Gauge Eastern 1”) and the U-jackets SGU3L (“Strain Gauge U-jacket Longitudinal”) as shown in Figure 6. The distribution of FRP strain along the beam soffit and the FRP strain at failure, i.e. the strain corresponding to the FRP rupture or debonding can be obtained.

4 Test results and analysis

The effects of bonding FRP strips to the beam soffit, adding U-jacket, vertical or inclined U-jacket, U-jacket anchorage coverage and epoxy adhesive on the strengthening performance are discussed and analysed through testing six specimens. Table 4 summarises the key performance of each specimen. Failure modes including cracking, FRP debonding and FRP rupture are presented and the data including load-displacement and strain-time histories were recorded. The load-displacement curves of all beams are presented in Figure 7.

4.1 Control specimen

The control specimen without strengthening experienced a flexural failure with severe vertical cracks. Flexural cracking was symmetrical and hardly any abnormalities were observed, confirming the correctness of the test setup. The cracks first appeared at mid-span and extended towards the supports. They were all visually classified as flexural cracks with no shear cracks appearing at any point during the test. All flexural cracks were propagated vertically from the soffit of the beam as shown in Figure 8.

The control specimen achieved an ultimate applied load of 61.65 kN and a maximum deflection of 16.70 mm at the ultimate load.

4.2 Efficiency of the longitudinal strip

The specimen B150A strengthened with BFRP strips at the soffit exhibited a similar flexural cracking pattern to the control specimen as shown in Figure 9 (a). An ultimate applied load of 74.37 kN was achieved with a corresponding mid-span deflection of 18.5 mm. B150A yielded a strength gain of 20.63% over the control specimen. After the applied load peaked, B150A experienced intermediate debonding at the load of 71 kN and subsequently, complete debonding on the left side of the beam as shown in Figure 9 (b). The debonding was caused by the failure of the concrete cover layer as shown in Figure 9 (c and d). The strain gauges on the soffit strip of B150A recorded a maximum strain of 0.96%, which was equal to 45.7% of the rupture strain from the BFRP coupon tests. As shown in Figure 10, the maximum FRP strain at the mid-span of 0.96% was recorded before debonding initiated and propagated from the mid-span. This FRP strain of 0.96% was thus considered as the debonding strain. This debonding strain was much higher than that of CFRP strengthened RC beams as reported by Fu et al. (2016), where the debonding strain was recorded as 0.2%.

4.3 Efficiency of U-jacket anchors

To examine the efficiency of using U-jackets as anchorage, the specimen B150B was prepared and tested. As shown in Figure 11, prior to failure, B150B experienced less severe cracking and better concrete confinement than B150A. As shown in Figure 7, an ultimate applied load of 84.9 kN with the corresponding deflection of 37.6 mm were recorded, which represented a significant flexural strength gain of 37.7% over the control specimen. Up to the ultimate load of B150A (i.e. 74.4 kN), B150B exhibited a similar load-displacement curve, indicating a similar stiffness as Beam B150A. Beyond this point, more deflection was achieved on B150B before failure, indicating the U-jackets provided additional ductility. Beam B150B (with U-jackets) had a strength increase of 14% over Beam B150A (without U-jackets). This increase agreed well with experimental results from the studies by Ceroni and Pecce [33] and Brena, et al. [34], where using CFRP U-wraps increased the strength capacity from 10% to 57%. As shown in Figure 12, at an applied load of 84 kN, the strain gauge SGC recorded a strain of over 1.8%, indicating that 85.7% of the BFRP's elongation strain capacity was utilised. This data demonstrated BFRP yielded excellent elongation strain efficiency. As shown in Figure 11, B150B experienced debonding of U-jackets before the mid-span rupture of the soffit strip occurred at approximately 82.9 kN. This failure mode demonstrated the effectiveness of the U-jackets in preventing the soffit strip from debonding. The rupture of the longitudinal FRP strip instead of FRP debonding was observed in the testing, indicating the BFRP material can be used more efficiently.

4.4 Efficiency of inclined U-jacket anchors

Beam B150C was prepared to investigate the effectiveness of using 45° inclined U-jackets. B150C was well confined with minimal cracking as shown in Figure 13. The propagation of the flexural cracks in B150C was slow and not as widespread as B150B. Prior to failure of the BFRP, minor flexural cracks appeared and were all less than 1mm wide. B150C experienced compressive failure of concrete on the upward face of the beam around the loading plate. As shown in Figure 7, B150C was significantly less ductile than B150B as it experienced plastic deformation for a smaller range of displacement before reaching the ultimate load. The stiffer behaviour of B150C was visually apparent during the test, as it appeared to be minimally deformed and very well confined throughout. Even after failure, B150C sustained a higher constant load between 61kN and 63kN until the test stopped. The higher residual strength of Beam B150C may be attributed to the inclined U-jackets which were still well attached on the beam soffit and transferred tensile stresses to the beam sides. Of all the tested beams, B150C recorded the highest ultimate load of 95.68 kN with a corresponding deflection of 22.9 mm shown in Figure 7, which represented a strength gain of 55.2% over the control beam and a 12.7% improvement with respect to B150B reinforced with vertical U-jackets. This result was consistent with the findings of Pham and Hao [29], who attributed the high strength associated with 45° inclined U-jackets to their enhanced ability to arrest flexural and shear cracks. In addition, placing the U-jackets at 45° meant that there was a slightly larger area of

BFRP bonded to the concrete and hence offered more resistance to the forces exerted by the soffit strip.

In the course of testing B150C, cracking noises could only be heard after the applied load exceeded 90 kN. When the applied load approached 95 kN, the cracking noises intensified, indicating that failure was imminent. When the applied load peaked at 95.68 kN, a strain of 1.68% was recorded in the BFRP before mechanical destruction of SGC occurred at 1.98% as shown in Figure 14. The strain of 1.98% and 1.68% represented 94.3% and 80% of the rupture strain of the BFRP, respectively, which indicated that BFRP material had an enhanced ability to exploit its high tensile strength before debonding or rupture. After the applied load peaked and gradually dropped to approximately 89 kN, the cracking noises intensified and a distinct tearing noise was heard. The observation of the beam revealed that the BFRP soffit strip ruptured completely at mid-span as shown in Figure 13 (c). Partial rupture of the soffit strip at the location of SGE3 (between inclined U-jackets East 4 and 5) was observed as shown in Figure 13 (d). It was worth mentioning that all the inclined U-jackets were still well attached to the beam sides while vertical U-jackets debonded in Beam B150B. The failure mode showed that utilizing U-jackets could effectively prevent premature debonding and induce BFRP rupture mode, which was owing to the effective anchorage of the BFRP soffit strip by the 45° inclined U-jackets, leading to the more efficient exploitation of the tensile strength of BFRP.

4.5 Efficiency of U-jacket anchors at mid-span only

B150D with partial U-jackets anchorage coverage was prepared to investigate the effect of U-jackets anchorage coverage on the strengthening performance. Aside from the relatively late appearance of flexural cracks, B150D exhibited a symmetrical cracking pattern. An ultimate load of 82.26 kN and deflection at ultimate load of 19.4 mm were recorded. B150D with partial anchorage exhibited a 33.4% flexural strength gain over the control beam and a 3.1% flexural strength loss to B150B with full U-jackets anchorage. This loss in flexural strength was considered to be minor, indicating that the U-jackets located on the outer thirds of the beam contribute minimally to the enhancement of flexural strength as compared to B150B. However, owing to the widespread confinement and anchorage offered by the U-jackets applied along the whole clear span of B150B, B150B was significantly more ductile than B150D prior to failure as revealed in the load-displacement curves of Figure 7. In addition, SGE2 out of the region of the U-jacket experienced higher strain than that of SGE2 in Beams B150B and B150C. It showed that the U-jackets distributed at 1/3 span near the support help to control the strain and longitudinal stress near the support. It is, therefore, concluded that using U-jackets for the whole beam span can significant delay the debonding and increase the ductility, although it only marginally increases the loading capacity of the beam strengthened with U-jackets only in the mid-span region.

At an applied load of approximately 76 kN, B150D experienced debonding of the soffit strip, followed by the complete debonding of U-jacket West UW2 and rupture of U-jacket West UW1 as shown in Figure 15 (b/c). In order to classify the type of debonding, BFRP samples were cut away from the soffit strip and U-jackets. As shown in Figure 16 (a), the debonding of BFRP soffit strip occurred within the concrete at the BFRP/concrete interface, indicating epoxy strength was higher than the concrete tensile strength. Figure 16 (b) shows the U-jacket removed from the beam. The U-jackets experienced the failure mode of severe concrete cover separation, evidenced by the large pieces of concrete substrate attached on the removed U-jackets, indicating the U-jackets can effectively transfer stress in the longitudinal BFRP strip to the beam sides. The failure of the concrete cover separation was attributed to the development of severe flexural cracks. A maximum soffit strain of 1.19% was recorded by the strain gauge SGE3 as shown in Figure 17.

4.6 Efficiency of different adhesives

To study the effect of adhesives on the strengthening performance, Beam B330B with the same wrapping scheme as B150B but using SikaDur 330 epoxy adhesive was prepared. As shown in Figure 18, B330B exhibited severe cracking before failure and no shear cracks were observed throughout the test. An ultimate load of 86.53 kN was achieved with a corresponding mid-span deflection of 36.3 mm. These values were close to the corresponding values of B150B. The flexural strength increase was 40.4%

and 1.9% over the control beam and Beam B150B, respectively. The strength gain over B150B was found insignificant and can be treated as a variation in the experimental tests. B330B and B150B had similar load-displacement curves until failure occurred on B150B. The key difference between these two beams was the higher ductility of B330B, which allowed deflecting approximately 25% more than B150B before failure. However, it was expected that the beam B330B strengthened with SikaDur 330 adhesive of higher tensile modulus should have yielded lower ductility, but the tests results were opposite. The reason for this observation is not exactly clear yet. Further study to confirm and explain the observed influences of different epoxies are deemed necessary. Based on the testing observation in this study, the increased ductility of B330B by using SikaDur 330 epoxy adhesive is a favourable characteristic for FRP-concrete composites.

At the applied load of 85 kN, B330B experienced intermediate debonding at three separate points along the soffit. Subsequently, UE5 began to debond and UE4 ruptured at the edge of the beam. This was followed by explosive debonding of the soffit strip on the right side, resulting in the rupture of UE1, UE2 and UE3. As shown in Figure 19, close examination of cut-outs from the debonded BFRP soffit strip and U-jackets revealed a generally pure adhesive failure at the BFRP concrete interface, leaving minimal damage to the concrete substrate.

B330B recorded a lower ultimate strain due to the lower tensile elongation capacity of the SikaDur 330 epoxy resin. A maximum strain of only 1.4% and strain efficiency of

66.6% were recorded as shown in Figure 20. This fell short of 1.8% strain and 85.7% strain efficiency of B150B. This was validated by the failure modes of B150B and B330B. B150B failed by the BFRP rupture while B330B failed predominantly by BFRP debonding. Due to the 4.5% tensile elongation capacity of the West System 105-206 epoxy applied to B150B being greater than the 2.1% tensile elongation capacity of the BFRP, the BFRP soffit strip of B150B failed once 2.1 % strain was exceeded. The relatively lower 0.9% tensile elongation capacity of the SikaDur 330 caused B330B BFRP debonding before the BFRP rupture. In general, the tested beams failed by the FRP rupture or the debonding of the concrete cover layer, indicating that the bonding strain of both adhesives were good.

5 Discussions and comparisons

5.1 Failure modes and load-displacement curves

All beams failed in the flexural mode. As demonstrated by the severe flexural cracking, the control beam without strengthening failed in flexural tension. Beams B150C and B150B failed in the form of BFRP strip rupture at mid-span soffit. This was largely due to the sufficient anchorage supplied by the U-jackets which enabled the beams to take advantage of the high tensile strength of BFRP. The rupture failure of Beams B150B and B150C was demonstrated by high exploitation of the BFRP's 2.1% rupture strain and the sudden mechanical failure of the respective strain gauges. Beams B150A, B150D and B330B failed in BFRP debonding of soffit strips. The mechanism observed for all debonding was classified as failure of the concrete cover layer. The debonding failure of Beams B150A, B150D and B330B was represented by the low utilization of available rupture strain capacity of BFRP. Despite being strengthened in the same wrapping scheme, Beams B330B and B150B experienced different failure modes due to the lower elongation capacity and the higher tensile modulus of SikaDur 330 epoxy adhesive as compared to those of West System 105-206.

The mid-span load-displacement curves of all tested beams were compared as shown in Figure 7. Comparisons between the elastic deformation of the control beam and that of the strengthened beams revealed that the contribution of the BFRP was activated at approximately 40 kN (about 67% of the capacity of the reference beam). Beyond the BFRP activation point, all strengthened beams were stiffer than the control beam. A dramatic drop in strength was observed for all strengthened beams immediately after the failure of BFRP. With respect to the ultimate load sustained by the control beam, B150A, B150B, B150C, B150D and B330B exhibited flexural strength gains of 20.6%, 37.7%, 55.2%, 33.4% and 40.4%, respectively. The wrapping scheme C offered the greatest strength gain due to the enhanced ability of inclined U-jackets to intercept severe shear and flexural cracks, which demonstrated the effectiveness of BFRP U-jackets in anchoring the soffit strip and delaying debonding. During the phase of plastic deformation, B150A, B150C and B150D showed relatively low ductility. However, both B150B and B330B demonstrated higher ductility than others and B330B exhibited the most ductile behavior among all beams, which indicated epoxy adhesive had a more significant effect on ductility and deformability than flexural strength.

5.2 FRP strain

The strain-time curves of the beams revealed strain values with respect to the BFRP's ultimate strain of 2.1%. BFRP was not exempted from the inefficient exploitation of FRP tensile strength that was commonly associated with the debonding failure linked to CFRP, GFRP and AFRP. After close examination, all instances of debonding were classified as failure of the concrete/BFRP interfacial and the epoxy adhesive. B150B and B150C failed by the rupture of the longitudinal BFRP strips. It was reflected by the high strains recorded by both beams, with B150B using a remarkable 95.7% of the available rupture strain prior to the rupture at 2.1%. Despite their similar wrapping schemes, B150B and B330B experienced different failure modes due to different elongation strain capacity and tensile modulus of epoxy used in the two beams, as discussed previously. SikaDur 330 failed before the BFRP could rupture. It should be noted that the debonding strain can be up to 1.19% by using BFRP and U-jacket anchorages, which was much higher than 0.4~0.6% by using CFRP as reported in the study [28]. The advantage of using BFRP as an alternative strengthening material was presented. It should be noted that the debonding stress corresponding to the debonding strain can be used in section analyses. The corresponding stress was calculated based on bond strength model, e.g., Teng et al.'s (2003) model [23] as adopted by ACI 440.2R-08 [30]. More details and discussion can be found in the previous study by Fu [35].

To examine the contribution of the U-jackets, strain gauges were bonded to the U-jackets in two directions as shown in Figure 10, Figure 12, Figure 14, Figure 17 and Figure 20. Vertical U-jackets dedonding at failure was observed in Beams B150B and B150D and vertical U-jackets ruptured in Beam B150D leading to the debonding in the longitudinal strip as shown in Figure 15 (c). Interestingly, all the inclined U-jackets of Beam B150C did not debond or rupture but the longitudinal FRP strip ruptured, indicating the superior performance of inclined U-jackets. In Beam B150B, the longitudinal and transverse strains of the debonded U-jacket (i.e. SGU5L and SGU5T) were approximately 0.4% and 0.3%, respectively. Meanwhile, the maximum longitudinal strain of the inclined U-jacket of Beam B150C was recorded as about 0.5% at SGU5L. This higher value of the longitudinal strain of the inclined U-jacket compared to the vertical U-jacket resulted in higher load-carrying capacity of Beam B150C than that of Beam B150B. U-jackets have proven their ability to delay the debonding of longitudinal strips. However, if the number of U-jacket anchors was not enough to transfer stress in longitudinal strips to the beam side, they might fail in shear in Beam B150 D as shown in Figure 15. The maximum transverse strain in vertical U-jackets was recorded as high as 1.19% as shown in Figure 17. Therefore, it again showed the advantage of using inclined U-jackets, where a portion of transverse stress caused by the deformation of the longitudinal strip can be resisted by the U-jacket in its longitudinal direction. In addition, ductility index, which is defined as the mid-span deflection at failure divided by the mid-span deflection at the yielding of steel tension bars, was used to quantify the ductility of beams [35]. As given in Table 4, the ductility index for the specimens B150A, B150B, B150C, B150D and B330B were 2.16, 3.32, 2.43, 2.23 and 4.08, with the increase of 3.8%, 59.6%, 16.8%, 7.2% and 96.2% over the control beam, respectively.

5.3 Efficacy comparison with CFRP

To compare the efficacy of using CFRP and BFRP, the beam design in this study was approximately the same as that in the study by Pham and Hao [28]. The efficacy of BFRP for the flexural strengthening of RC beam was therefore compared with CFRP strengthened beams by Pham and Hao [28]. Four layers of longitudinal BFRP strips were applied to ensure the equal tensile force (i.e. cross section*tensile strength) provided by two layers of CFRP strips. The BFRP/CFRP-strengthened beams showed the maximum loads 84.9 kN and 86.6 kN, respectively. These two strengthened beams also showed similar stiffness until failure as shown in Figure 21. It is noted that the energy absorption is defined as the area under the load-displacement curves of the beams up to failure of the longitudinal strips (i.e. a significant drop in the curves) since the contribution of FRP to the strengthened beam's capacity is of interest in this study. The energy absorptions of BFRP and CFRP-strengthened beams at the ultimate loads were 2.4 kNm and 3.2 kNm, respectively. However, BFRP has great potential as strengthening material compared to other materials (e.g. CFRP, GFRP, and AFRP) due to its cost-effectiveness.

6 Verification against guideline

The guideline ACI 440.2R-08 [30] is adopted for analytical verification to predict the ultimate moment capacity (Mu) of a beam with wrapping scheme A (i.e. B150A). To make comparisons between the analytical and experimental results, the ultimate applied load recorded in the tests is expressed as the ultimate bending moment, which is 33.48 kNm. Currently, ACI 440.2R-08 [30] is only applicable to CFRP, GFRP and AFRP materials and the wrapping scheme A. The predication on load carrying capacity of B150A using ACI 440.2R-08 is expressed as follows:

$$Mu = 0.85f'_c b\beta c \left(c - \frac{\beta}{2}c\right) + A'_s E_s \varepsilon'_s (c - d_c) + A_s f_y (d - c) + \Psi A_f E_f \varepsilon_{db} (h - c) \quad (1)$$

where $\boldsymbol{\Psi}$ is the reduction factor on the contribution of FRP to beam strength, β is a coefficient defined in ACI318-08 [36] , c is the depth of concrete compression block; A_f , A_s and $A_s^{'}$ represent the cross section area of FRP reinforcement, tension rebar and compression rebar, respectively; ε_s and $\varepsilon_s^{'}$ represent the strain in tension rebar and compression rebar; ε_{db} stands for debonding strain of FRP.

The ultimate moment capacity predicted by ACI 440.2R-08 [30] is 31.1 kNm, which underestimates the testing ultimate moment capacity (Mu) by 7%, with an error margin less than 10%. Therefore, the beam using wrapping scheme A with BFRP composites can yield reasonably sound prediction by using ACI 440.2R-08 [30]. ACI 440.2R-08 also gives the prediction of the FRP debonding strain (ε_{fd}) of B150A as follows:

$$\varepsilon_{fd} = 0.41\sqrt{\frac{f_c^{'}}{nE_f t_f}} \leq 0.9\varepsilon_{fu} \tag{2}$$

where $f_c^{'}$ is the compressive stress in concrete; n is the number of plies of FRP reinforcement. E_f and t_f represent tensile modulus and nominal thickness of one ply of FRP reinforcement. After calculation, the FRP debonding strain ε_{fd} is 1.32%. In the tests, the FRP debonding strain of B150A was measured as 0.96 %, which is lower than the value predicted by ACI 440.2R-08 [30].

7 Conclusions

This study presents the performance of RC beams strengthened with BFRP against quasi-static loading. The experimental results show that external bonding of BFRP sheets is an effective method of enhancing flexural strength of reinforced concrete beams. Failure mode is highly dependent on the degree of anchorage offered by the wrapping schemes and the mechanical properties of the epoxy adhesive. The findings in this study are summarized as follows:

1. Using U-jackets as an anchor system can change the failure mode from FRP debonding to FRP rupture. By using the same amount of materials, inclined U-jackets (highly recommended) is much more efficient than vertical U-jackets.

2. Using U-jackets anchorage is able to provide significant anchorage and delaying debonding by increasing the load-carrying capacity of B150A from 20% to 37.8% of B150B with U-jackets anchorages.

3. Full coverage of U-jackets anchorage performs slightly better than partial coverage of U-jackets anchorage by enhancing the load-carrying capacity of B150D from 33.4% to 37.8% of B150B with full coverage of U-jackets anchorages.

4. Using inclined U-jackets is more effective than vertical U-jacket with the load-carrying capacity increased from 37.7% of B150B to 55.2% of B150C anchored with inclined U-jackets.

5. The Beam B330B with SikaDur 330 adhesive has slightly higher load-carrying capacity but less ductility than the Beam B150B with West System 105-206 adhesive.

6. ACI 440.2R-08 predicts the ultimate moment capacity of B150A with error margin of 7% and the formulae were therefore deemed applicable to BFRP strengthened beam at the soffit.

In addition, as evidenced by the recorded high strain values, BFRP shows its ability to make use of its high tensile strength more efficiently than carbon, glass and aramid FRPs. Coupled with its low price, excellent heat resistance and lower environmental impact, the use of BFRP for flexural strengthening of RC structures is justifiable and ideal where the very high tensile strength of CFRP is not necessary. After the current quasi-static study, the performance of RC beams strengthened with BFRP sheet subjected to dynamic loading will be investigated to have a more comprehensive understandings of the effectiveness of BFRP strengthening of concrete beams subjected to both static and dynamic loads.

Acknowledgements

The authors would like to acknowledge Australian Research Council (Grant No. LP150100259) for financial support to carry out this study. The authors also acknowledge the technical support from Arne Bredin, Mick Ellis, Ashley Hughes, Luke English, Rob Walker, and Craig Gwyther at Curtin University.

References

[1] M. Erki, U. Meier, Impact loading of concrete beams externally strengthened with CFRP laminates, J. Composite Constr., 3 (1999) 117-124.

[2] L. Huang, B. Yan, L. Yan, Q. Xu, H. Tan, B. Kasal, Reinforced concrete beams strengthened with externally bonded natural flax FRP plates, Composites Part B: Engineering, 91 (2016) 569-578.

[3] J. Dong, Q. Wang, Z. Guan, Structural behaviour of RC beams with external flexural and flexural–shear strengthening by FRP sheets, Composites Part B: Engineering, 44 (2013) 604-612.

[4] E. Choi, N. Utui, H.S. Kim, Experimental and analytical investigations on debonding of hybrid FRPs for flexural strengthening of RC beams, Composites Part B: Engineering, 45 (2013) 248-256.

[5] T. Skuturna, J. Valivonis, Experimental study on the effect of anchorage systems on RC beams strengthened using FRP, Composites Part B: Engineering, 91 (2016) 283-290.

[6] Q.-Q. Yu, Y.-F. Wu, Fatigue Strengthening of Cracked Steel Beams with Different Configurations and Materials, J. Composite Constr., (2016) 04016093.

[7] T.H. Nguyen, X.H. Vu, A.S. Larbi, E. Ferrier, Experimental study of the effect of simultaneous mechanical and high-temperature loadings on the behaviour of textile-reinforced concrete (TRC), Constr Build Mater, 125 (2016) 253-270.

[8] V. Fiore, T. Scalici, G. Di Bella, A. Valenza, A review on basalt fibre and its composites, Composites Part B: Engineering, 74 (2015) 74-94.

[9] J. Sim, C. Park, D.Y. Moon, Characteristics of basalt fiber as a strengthening material for concrete structures, Composites Part B: Engineering, 36 (2005) 504-512.

[10] T.M. Pham, L.V. Doan, M.N.S. Hadi, Strengthening square reinforced concrete columns by circularisation and FRP confinement, Constr Build Mater, 49 (2013) 490-499.

[11] J. Teng, J.-F. Chen, S.T. Smith, L. Lam, FRP: strengthened RC structures, Frontiers in Physics, (2002).

[12] H. Rahimi, A. Hutchinson, Concrete beams strengthened with externally bonded FRP plates, J. Composite Constr., 5 (2001) 44-56.

[13] H. Saadatmanesh, M.R. Ehsani, RC beams strengthened with GFRP plates. I: Experimental study, J. Struct. Eng., 117 (1991) 3417-3433.

[14] S.T. Smith, J. Teng, FRP-strengthened RC beams. I: review of debonding strength models, Eng. Struct., 24 (2002) 385-395.

[15] T.M. Pham, H. Hao, Review of Concrete Structures Strengthened with FRP Against Impact Loading, Structures, 7 (2016) 59-70.

[16] T.C. Triantafillou, N. Plevris, Strengthening of RC beams with epoxy-bonded fibre-composite materials, Mater. Struct., 25 (1992) 201-211.

[17] G. Spadea, F. Bencardino, F. Sorrenti, R.N. Swamy, Structural effectiveness of FRP materials in strengthening RC beams, Eng. Struct., 99 (2015) 631-641.

[18] N. Attari, S. Amziane, M. Chemrouk, Flexural strengthening of concrete beams using CFRP, GFRP and hybrid FRP sheets, Constr Build Mater, 37 (2012) 746-757.

[19] T. Sen, J.H.N. Reddy, Strengthening of RC beams in flexure using natural jute fibre textile reinforced composite system and its comparative study with CFRP and GFRP strengthening systems, International Journal of Sustainable Built Environment, 2 (2013) 41-55.

[20] A. Şerbescu, P. Kypros, N. Ţăranu, The Efficiency of Basalt Fibres in Strengthening the Reinforced Concrete Beams, The Bulletin of the Polytechnic Institute of Jassy, Construction. Architecture Section, 52 (2006) 47-58.

[21] J. Bonacci, M. Maalej, Behavioral trends of RC beams strengthened with externally bonded FRP, J. Composite Constr., 5 (2001) 102-113.

[22] Yao, Teng, Lam, Experimental study on intermediate crack debonding in FRP-strengthened RC flexural members, Adv. Struct. Eng, 8 (2005) 365-396.

[23] J. Teng, S.T. Smith, J. Yao, J. Chen, Intermediate crack-induced debonding in RC beams and slabs, Constr Build Mater, 17 (2003) 447-462.

[24] A. Chahrour, K. Soudki, Flexural response of reinforced concrete beams strengthened with end-anchored partially bonded carbon fiber-reinforced polymer strips, J. Composite Constr., 9 (2005) 170-177.

[25] B. Fu, J.G. Teng, J.F. Chen, G.M. Chen, Y.C. Guo, Concrete Cover Separation in FRP-Plated RC Beams: Mitigation Using FRP U-Jackets, J. Composite Constr., (2016) 04016077.

[26] S.T. Smith, J.G. Teng, Shear-bending interaction in debonding failures of FRP-plated RC beams, Adv. Struct. Eng, 6 (2003) 183-199.

[27] J. Lee, M.M. Lopez, Characterization of FRP Uwrap Anchors for Externally Bonded FRP-Reinforced Concrete Elements: An Experimental Study, J. Composite Constr., 20 (2016).

[28] T.M. Pham, H. Hao, Behavior of FRP Strengthened RC Beams under Static and Impact Loads, Int J Protective Struct, (2016).

[29] T.M. Pham, H. Hao, Impact Behavior of FRP-Strengthened RC Beams without Stirrups, J. Composite Constr., 20 (2016).

[30] A.C. Institute, Guide for the Design and Construction of Externally Bonded FRP Systems for Strengthening Concrete Structures, in: ACI 440.2 R-08, American Concrete Institute, 2008.

[31] W. Chen, H. Hao, M. Jong, J. Cui, Y. Shi, L. Chen, T.M. Pham, Quasi-static and dynamic tensile properties of basalt fibre reinforced polymer, Composites Part B: Engineering, 125 (2017) 123-133.

[32] A. Mutalib, Damage assessment and prediction of FRP strengthened RC structures subjected to blast and impact loads, in, University of Western Australia, 2011.

[33] F. Ceroni, M. Pecce, Evaluation of bond strength in concrete elements externally reinforced with CFRP sheets and anchoring devices, J. Composite Constr., 14 (2010) 521-530.

[34] S.F. Brena, R.M. Bramblett, S.L. Wood, M.E. Kreger, Increasing flexural capacity of reinforced concrete beams using carbon fiber-reinforced polymer composites, ACI Struct J, 100 (2003) 36-46.

[35] B. Fu, Debonding failure in FRP-strengthened RC beams: prediction and suppression, in, The Hong Kong Polytechnic University 2016.

[36] ACI_Committee, Building code requirements for structural concrete (ACI 318-08) and commentary, in, American Concrete Institute, 2008.

ACCEPTED MANUSCRIPT

Table 1 Description of testing specimens

Specimen	Epoxy adhesive	Wrapping scheme	Wrapping scheme description
Control	N/A	N/A	N/A
B150A	West System 105-206	A	4 layer soffit strip
B150B	West System 105-206	B	4 layer soffit strip/ 2 layer vertical U-jackets throughout length
B150C	West System 105-206	C	4 layer soffit strip/2 layer 45° U-jackets throughout length
B150D	West System 105-206	D	4 layer soffit strip/ 2 layer vertical U-jackets central third of length
B330B	SikaDur 330	B	4 layer soffit strip/ 2 layer vertical U-jackets throughout length

Table 2 Mechanical properties of BFRP and CFRP materials

Parameter	300 g/m^2 BFRP	340 g/m^2 CFRP*
Width (mm)	100	75
Nominal thickness (mm)	0.12	0.45
Tensile strength (MPa)	1684	1500
Tensile force per layer	25200	50625
Failure strain %	2.1	1.65
FRP layers	4	2

*Data is adopted from the previous study [28].

Table 3 Mechanical properties of epoxy adhesives

Mechanical properties	SikaDur 330	West System 105-206
Required Curing (Days)	7 at 23°C	4 at 16°C
Tensile Strength (MPa)	30	50.3
Tensile Modulus (MPa)	4500	3171.6
Tensile Elongation (%)	0.9	4.5
Resin/ Hardener Mix Ratio	4:1 by Weight	5:1 by Volume

Table 4 Summary of testing data

Specimen	Control	B150A	B150B	B150C	B150D	B330B
Ultimate load (kN)	61.65	74.37	84.90	95.68	82.26	86.53
Load capacity increase (%)	-	20.6	37.7	55.2	33.4	40.4
Deflection at ultimate load (mm)	17.33	18.50	37.56	22.90	19.41	36.30
Deflection at the yielding of steel tension bars (mm)	8.04	8.54	11.30	9.41	8.70	8.90
Ductility index	2.08	2.16	3.32	2.43	2.23	4.08
Soffit debonding strain (%)	-	0.96	N/A	N/A	1.19	N/A
Max strain in soffit strip before failure (%)	-	0.96	1.80	1.68	1.19	1.40
Strain efficiency (%)	N/A	45.7	85.7	80.0	56.7	66.7

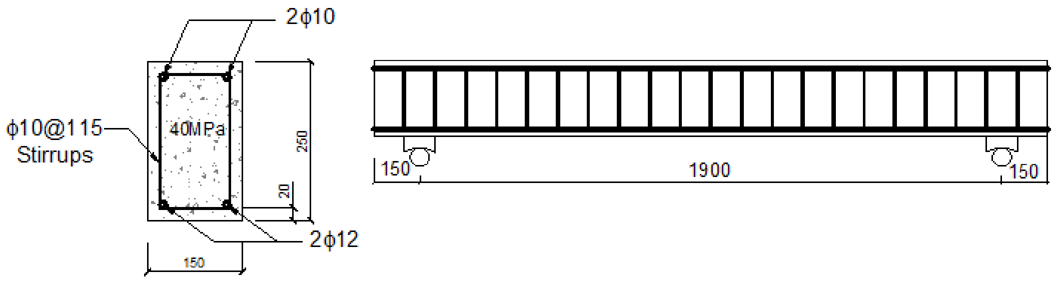

Figure 1 Dimension and configuration of RC beam

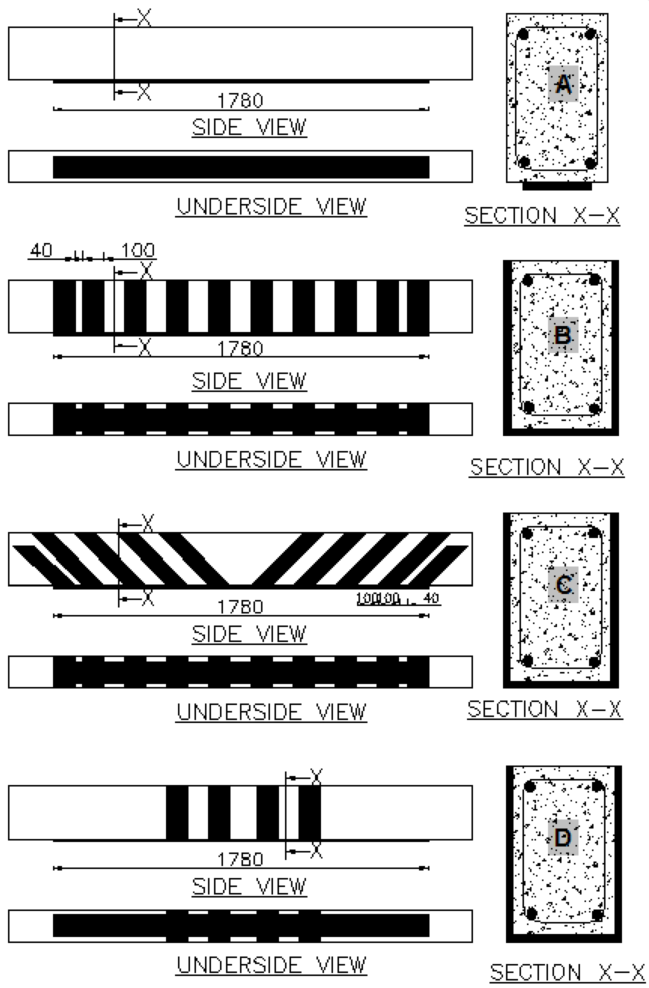

Figure 2 Wrapping scheme A/B/C/D

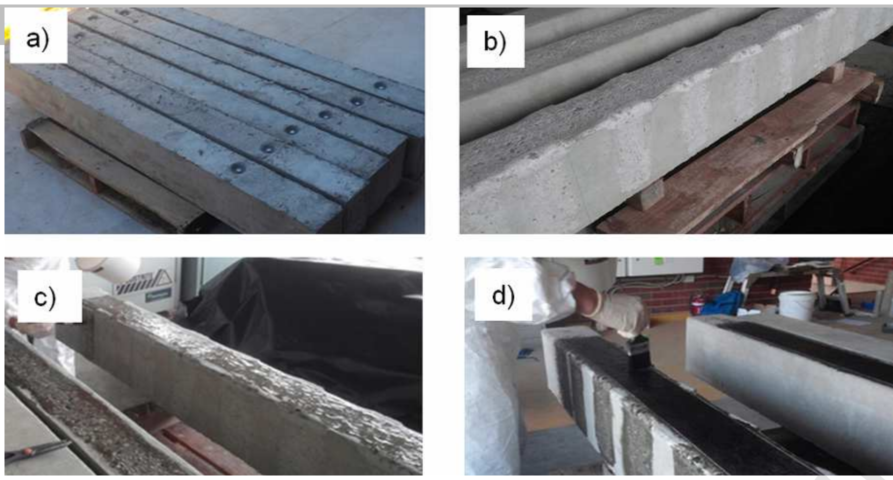

Figure 3 (a) Casted beams; (b) Edges rounded and surface roughened; (c) Priming of the roughened concrete surface (d) Wet layup of BFRP strips

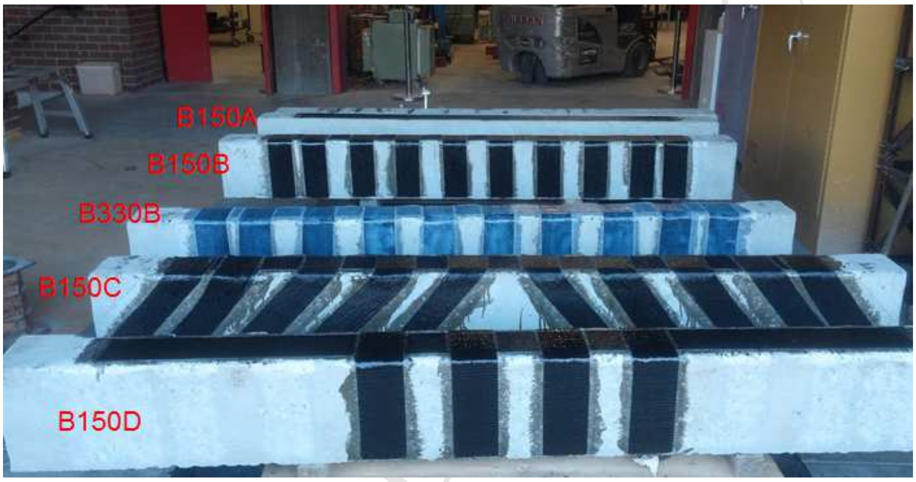

Figure 4 Testing specimens

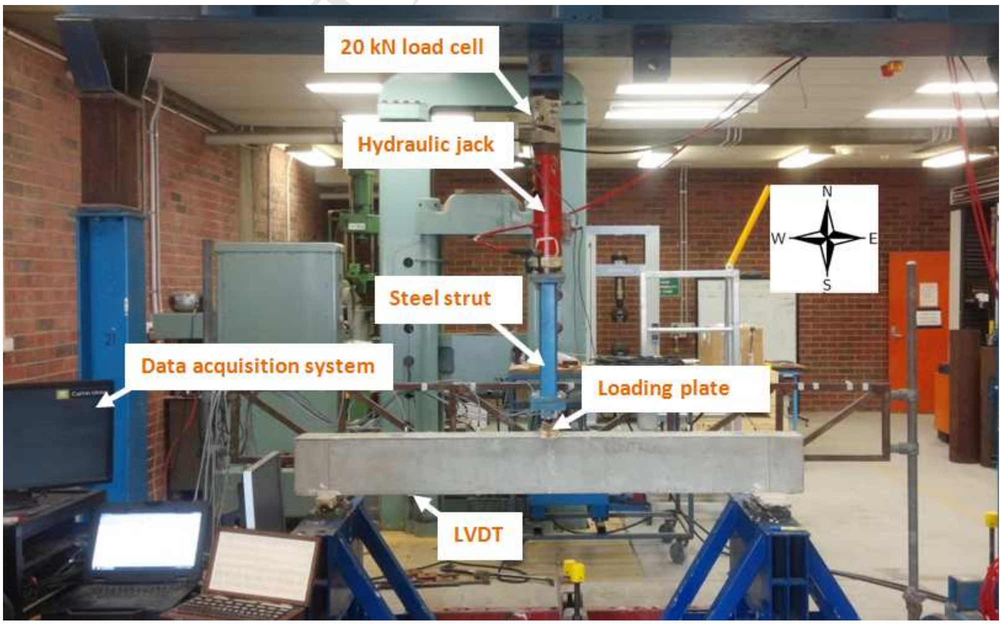

Figure 5 Three-point testing setup

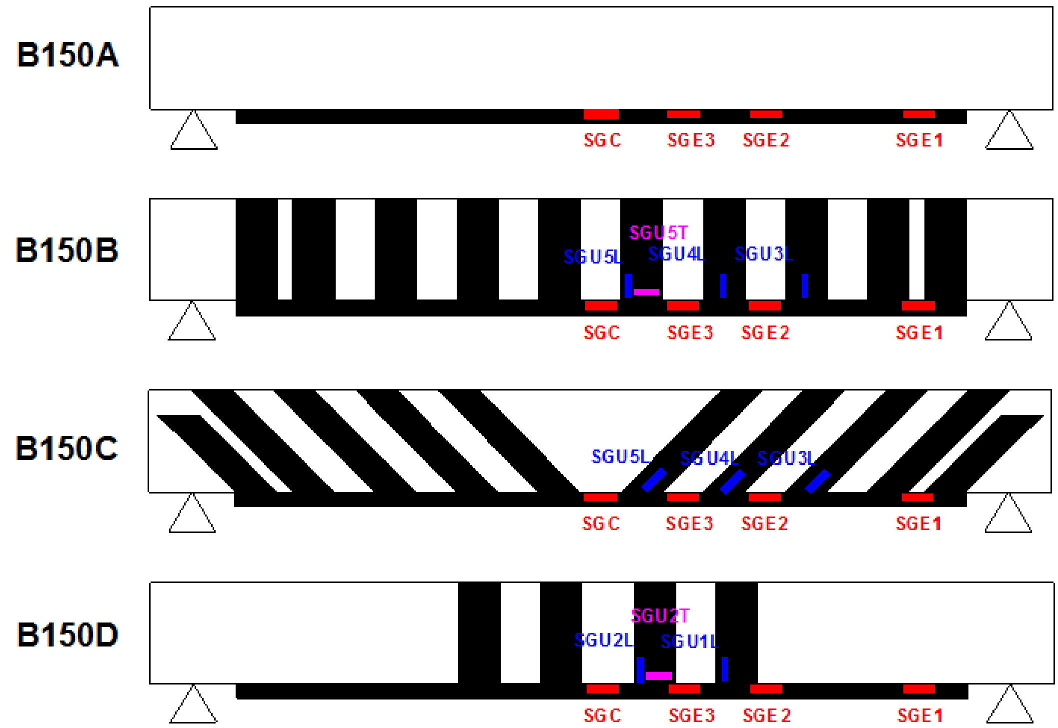

Figure 6 Installation of strain gauges

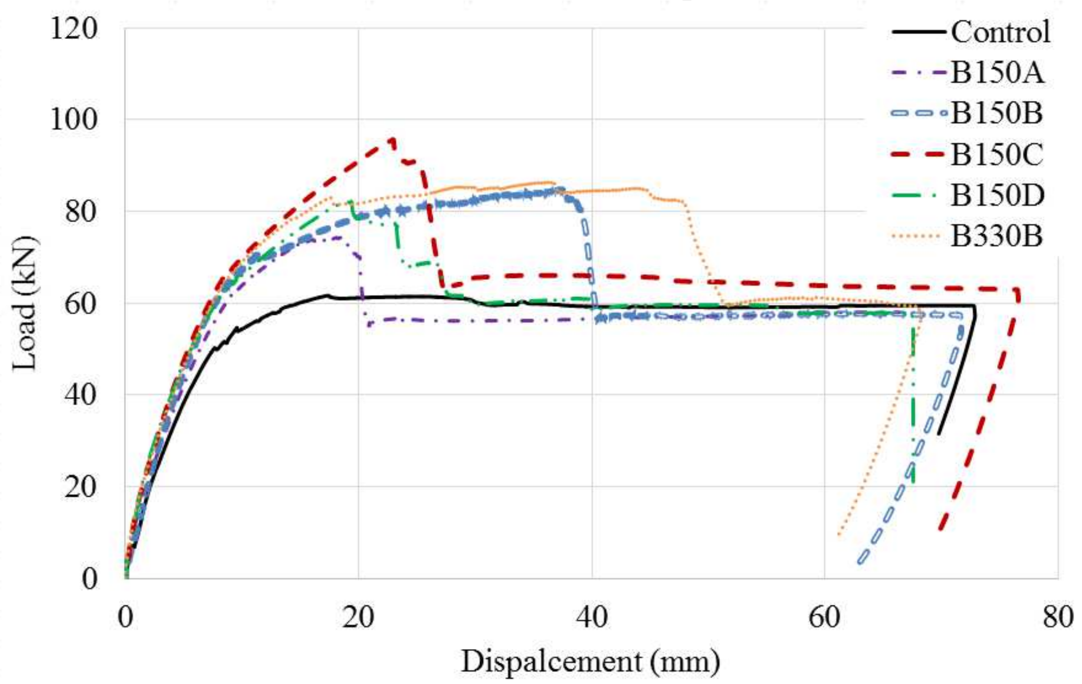

Figure 7 Load-displacement curves of all beams

Figure 8 (L) Early crack development of control specimen, (R) Crack development close to failure load of control specimen

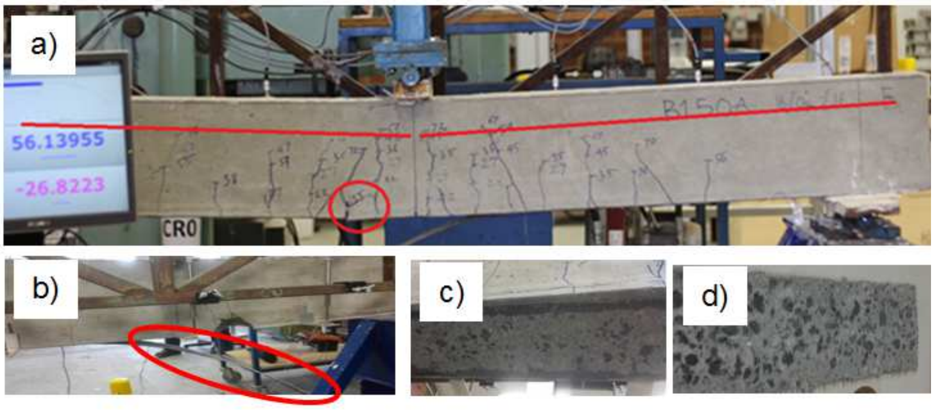

Figure 9 (a) Failure mode of specimen B150A (b) Debonded BFRP strip; (c) Concrete surface after debonding; (d) BFRP/concrete interface after debonding

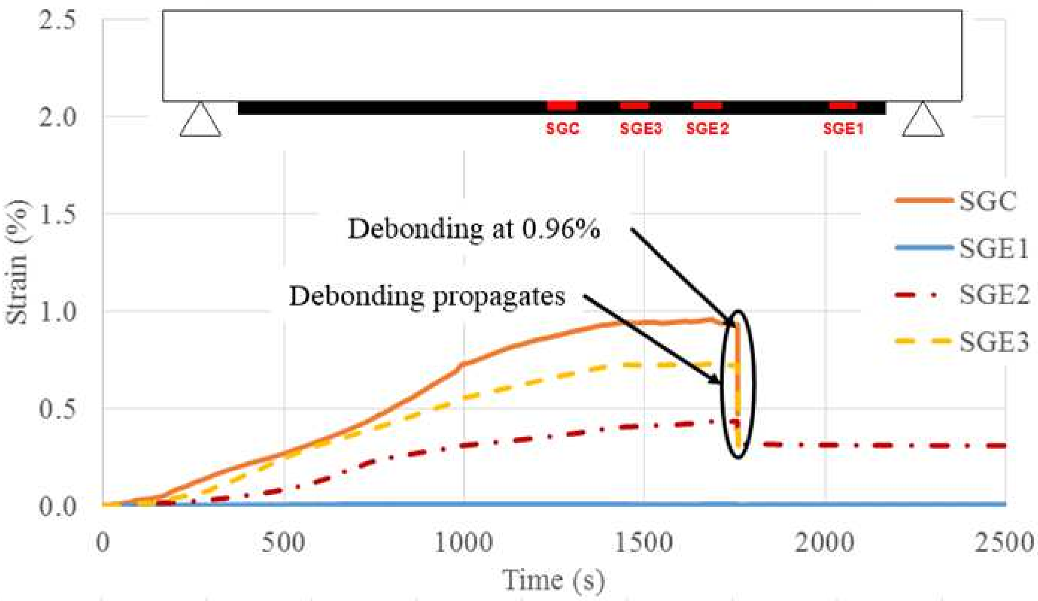

Figure 10 Strain-time histories of Beam B150A

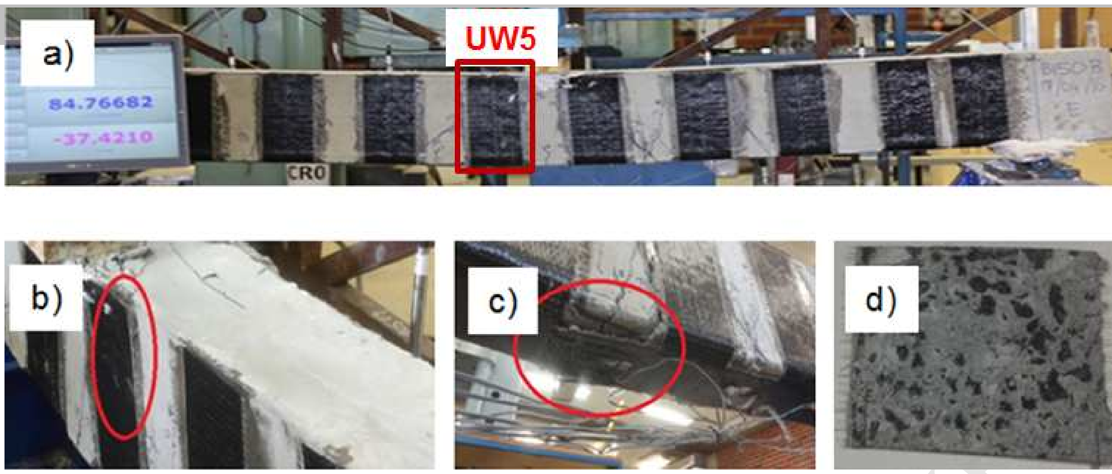

Figure 11 (a) Failure mode of Beam B150B; (b) U-jacket debonding; (c) Rupture of the soffit strip; (d) BFRP/Concrete interfacial failure of U-jacket UW5

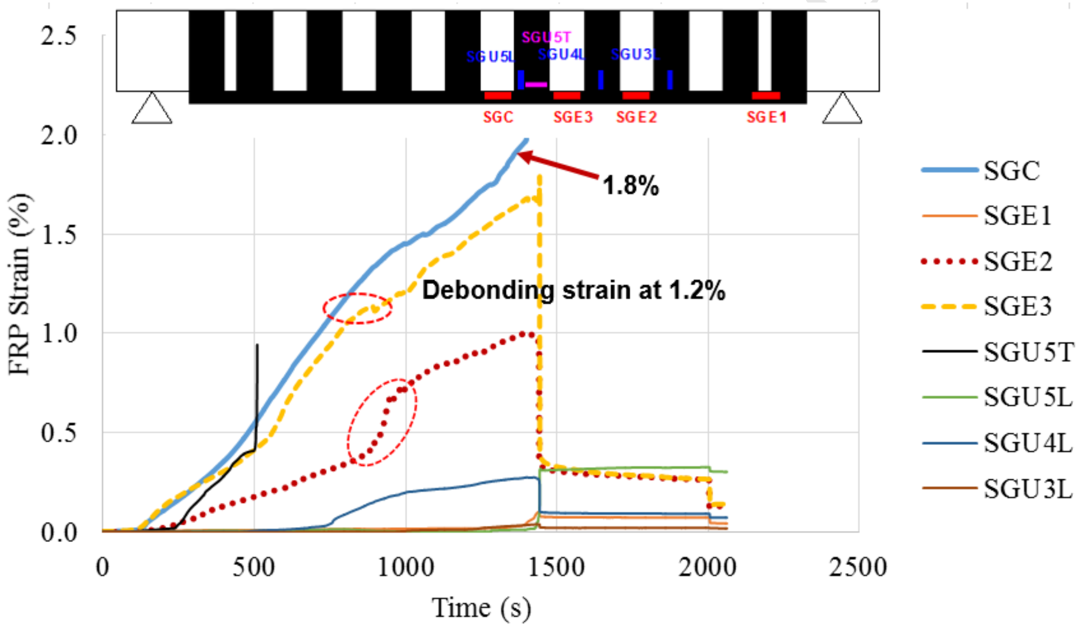

Figure 12 Strain-time histories of Beam B150B

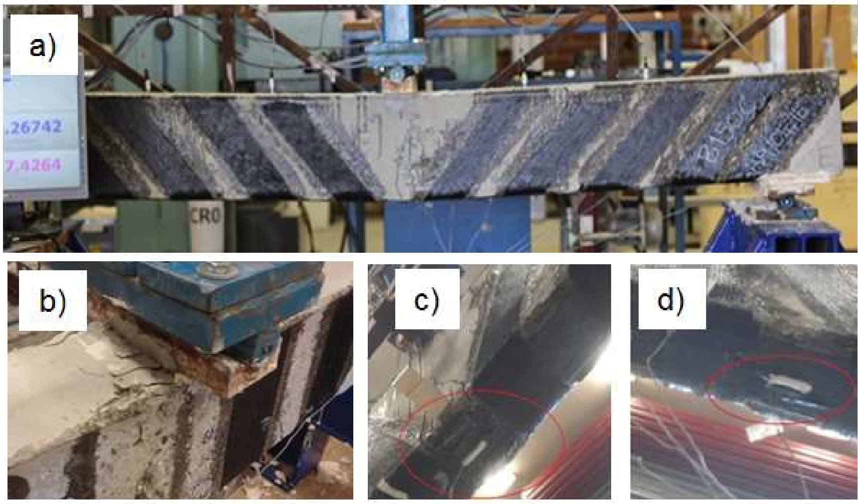

Figure 13 (a) Failure mode of Beam B150C; (b) Compressive failure of concrete at loading plate; (c) Complete BFRP rupture at mid-span; (d) Partial BFRP rupture at SGE3

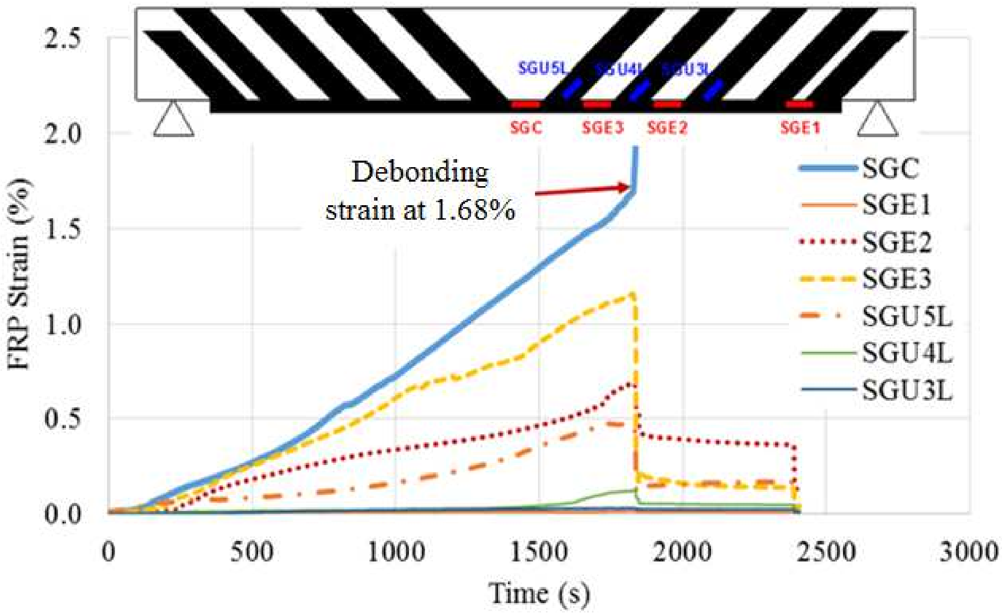

Figure 14 Strain-time histories of Beam B150C

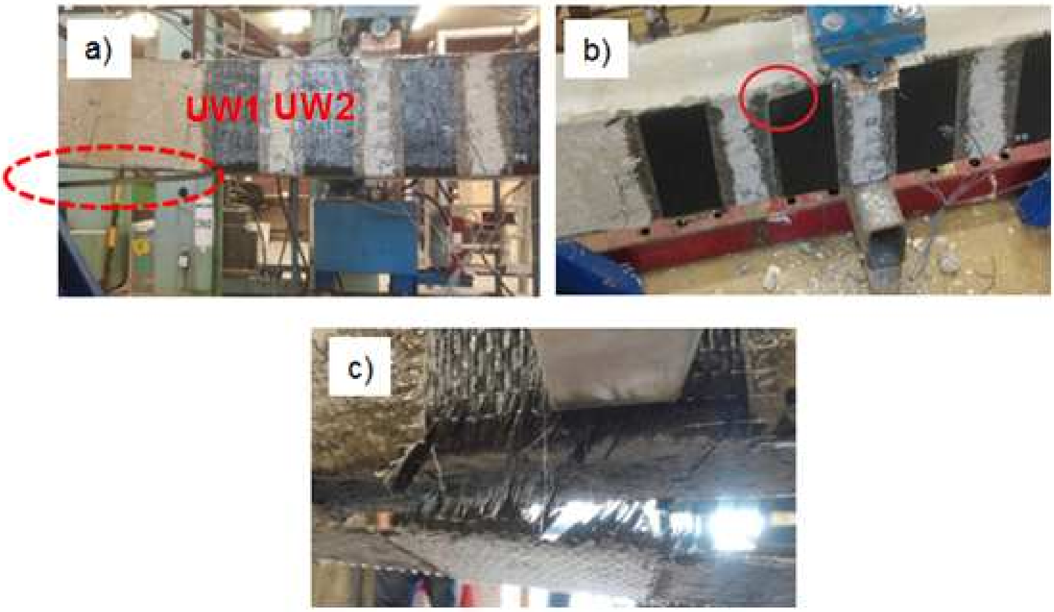

Figure 15 (a) Debonding of the BFRP soffit strip where no U-jacket anchorage; (b) Debonding of UW2 of B150D; (c) Rupture of UW1 at the edge of B150D

Figure 16 (a) Interfacial failure of the soffit strip, (b) Concrete cover separation of the U-jacket

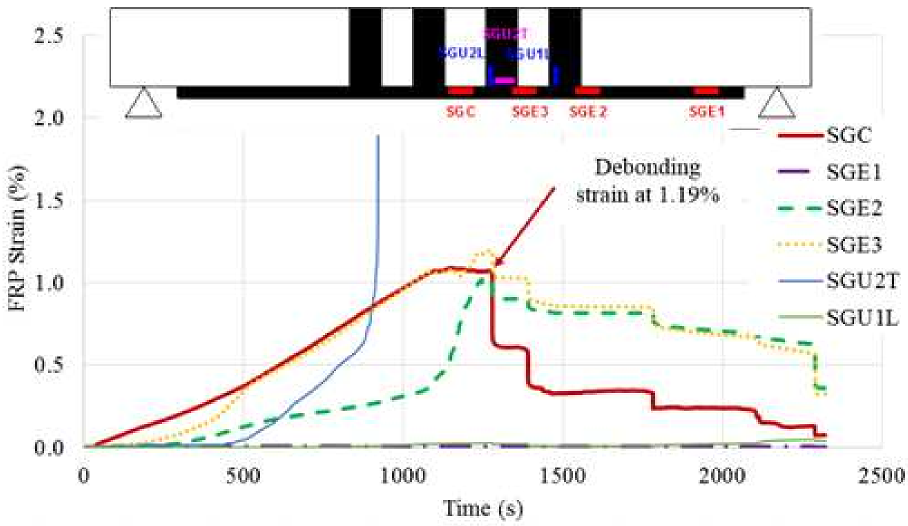

Figure 17 Strain-time histories of Beam B150D

Figure 18 (a) Intermediate crack induced interfacial debonding of soffit strip of B330B; (b) Complete failure of B330B by debonding of soffit strip and rupture of UE1, UE2 and UE3

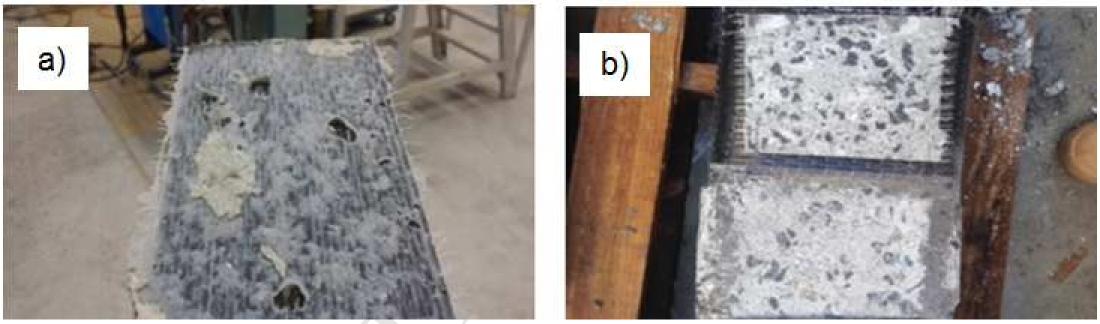

Figure 19 (a) Adhesive failure at BFRP/concrete interface of B330B, (b) Minimal damage to concrete substrate of B330B

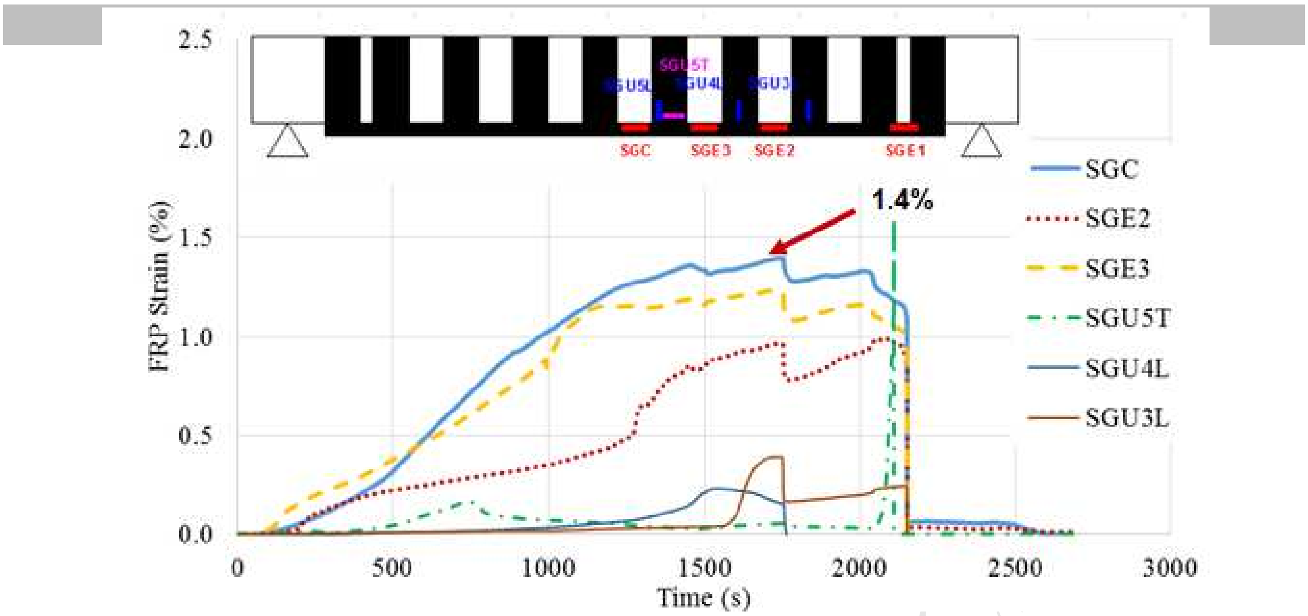

Figure 20 Strain-time histories of Beam B330B

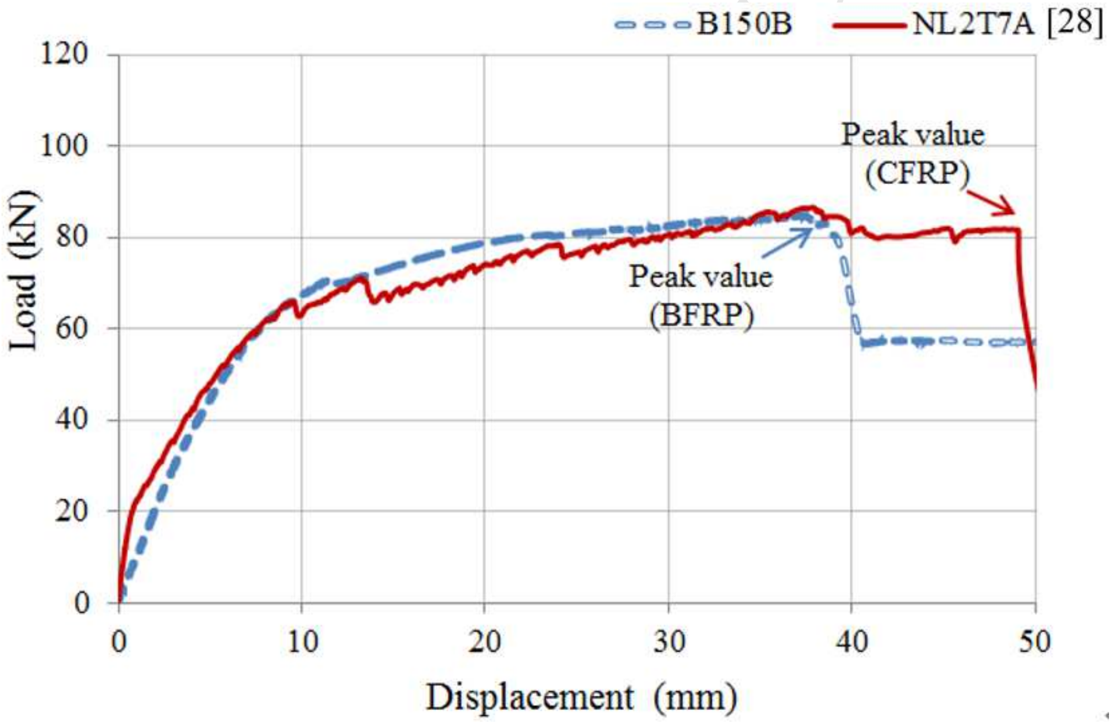

Figure 21 Load-displacement curves of BFRP strengthened beam B150B and CFRP strengthened beam NL2T7A [28]

- Very limited study on RC beams strengthened by BFRP is available.
- The effect of various BFRP wrapping schemes on the flexural performance is studied.
- The effect of U-jacket anchorage on BFRP strengthening performance is analyzed.
- The effect of epoxy adhesives on the flexural capacity of RC beams is investigated.
- The predication on BFRP strengthening by using ACI 440.2R-08 is verified.